Magnetic Instruments

Estimation of Angular Deviations in Precise Magnetometers

Michal Janosek[1]*, Elda F. Saunderson[2, 3], Michal Dressler[1]* and Daniel J. Gouws[2]
[1] Czech Technical University in Prague, Faculty of Elec. Eng., Dept. of Measurement, Praha, 16000, Czech Republic
[2] South African National Space Agency, Directorate Space Science, Hermanus, 7200, Republic of South Africa
[3] Dept. of Electrical and Electronic Engineering, Stellenbosch University, Stellenbosch, 7600, Republic of South Africa
* Member, IEEE

Received 1 Apr 2016, revised 15 Apr 2016, accepted 20 Apr 2016, published 1 Jun 2016, current version 15 Jun 2016.

Abstract— Capabilities for calibrations of angular deviations of sensor triplets in precise magnetometers were evaluated in a 2.5-meter, triaxial Helmholtz-coil facility. The coil system is located in a magnetically quiet environment at SANSA Space Science in Hermanus, South Africa. The angular calibration results obtained from the "thin-shell" calibration procedure were compared with direct measurements on a non-magnetic tilting/rotational platform. One-year expanded uncertainty of angular deviation calibrations is estimated as 6×10^{-2} degrees of arc; 3×10^{-4} degrees coil orthogonality is possible when doing a numerical re-calibration and correction on a short-term basis. In addition, an approach for obtaining body-to-sensor angular calibrations is presented, allowing for speed-up of the calibrations and possibly increasing their accuracy and repeatability by avoiding alignment to the coils with a laser beam and leveling.

Index Terms— Magnetic instruments, magnetometer calibrations, precision, uncertainty.

I. INTRODUCTION

Precise triaxial magnetometers require careful calibration to establish all nine parameters (gains, offsets, non-orthogonal angles) [Olsen 2003]; if the magnetometer is intended for navigation and data fusion with another physical sensor, three further parameters are needed to describe their (mutual) attitude [Primdahl 2002], [Vcelak 2009], [Figaro 2011].

SANSA Space Science in Hermanus, South Africa, operates a square, 2.5 m triaxial Helmholtz coil system for magnetic sensor calibrations - see Fig. 1. With the help of a LEMI-025 magnetometer at a distance of 40 m, it is possible to suppress local magnetic field variations occurring during the calibration run due to the high homogeneity of the Earth's magnetic field at the location (the site houses a magnetic observatory). Moreover, the on-site magnetic noise is less than 10 pT/$\sqrt{\text{Hz}}$ at 1 Hz, even during the day.

Fig. 1. The square triaxial coil system at SANSA.

Corresponding author: M. Janosek (janosem@fel.cvut.cz).
Digital Object Identifier: 10.1109/LMAG.XXXX.XXXXXXX (inserted by IEEE).

The coil system is mechanically leveled and calibrated on a periodic basis; the magnetic direction of the EW axis is aligned with a reference laser.

We present our current approach of calibrating the angular deviations, the results, estimation of the uncertainty, and a novel method of estimating the body-frame related calibration.

II. MAGNETOMETER MODEL AND CALIBRATION PROCEDURE

A. Magnetometer model

To express non-orthogonalities between magnetometer axes, we use the typical model as described by Olsen [2003] - see Fig. 2.

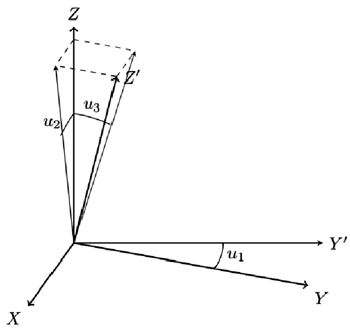

Fig. 2. The triaxial magnetometer sensor frame depicting the non-orthogonal angles u_1, u_2 and u_3 [Olsen 2003].

In this case, the X axis is assumed as reference, the non-orthogonal Y' axis is assumed to be in plane, only rotated by an angle u_1 from the X axis; i.e. the XY (XY') plane is the reference plane. Then the Z' axis is established by two non-orthogonal angles

u_2 and u_3 deviating from the ideal Z axis orthogonal to XY plane. The effect of non-orthogonality can be then expressed with a matrix **P** containing the angular deviations u_1, u_2 and u_3 [Olsen, 2003]:

$$\mathbf{P} = \begin{bmatrix} 1 & 0 & 0 \\ -\sin(u_1) & \cos(u_1) & 0 \\ \sin(u_2) & \sin(u_3) & \sqrt{(1-\sin^2(u_2)-\sin^2(u_3))} \end{bmatrix} \quad (1)$$

We can then establish the magnetic field vector $\mathbf{b}_{mag}$ from the magnetometer output vector $\mathbf{e}_{mag}$ by multiplying by it the inverse non-orthogonality matrix $\mathbf{P}^{-1}$ and the inverse sensitivity matrix $\mathbf{S}^{-1}$, after subtracting the offset vector $\mathbf{e}_o$ in arbitrary (engineering) units.

$$\mathbf{b}_{mag} = [\mathrm{b}_{magX}\ \mathrm{b}_{magY}\ \mathrm{b}_{magZ}]^{\mathbf{T}} = \mathbf{P}^{-1}\mathbf{S}^{-1}(\mathbf{e}_{mag} - \mathbf{e}_{\mathbf{o}}) \quad (2)$$

So far the calibration is considered to an x-axis referenced frame ("sensor frame"), which can differ from the mechanical enclosure of the magnetometer ("body frame") - see Fig. 3 - which is positioned in the frame of the coil system ("global frame").

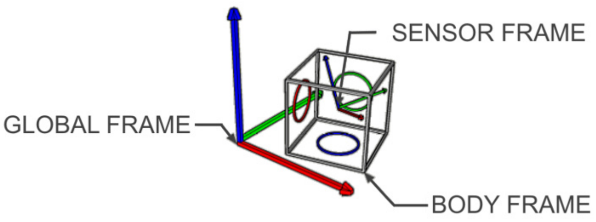

Fig. 3. Definition of the magnetometer sensor frame, magnetometer body frame and global frame (=coil frame).

To be able to fully describe the measured field with reference to the magnetometer body frame, we need to add an additional rotational matrix **R** describing the rotation of the sensor frame to the body frame. $\mathbf{R}^{-1}$, $\mathbf{P}^{-1}$, and $\mathbf{S}^{-1}$ can be combined to a single matrix **A**:

$$\boldsymbol{b}_{mag} = \boldsymbol{R}^{-1}\boldsymbol{P}^{-1}\boldsymbol{S}^{-1}(\boldsymbol{e}_{mag} - \boldsymbol{e}_{o}) = \boldsymbol{A}(\boldsymbol{e}_{mag} - \boldsymbol{e}_{o}) \quad (3)$$

B. Calibration Procedure

The calibration procedure relies generally on solving an overdetermined system of equations (2), i.e. the $\mathbf{b}_{mag}$ is created by the coil system, $\mathbf{e}_{mag}$ is measured, and the $\mathbf{R}^{-1}\mathbf{P}^{-1}\mathbf{S}^{-1}$ matrix can be established, or even the components of **P** matrix (2) individually to obtain the non-orthogonal angles u_1, u_2 and u_3. The test field vector $\mathbf{b}_{coil}$ is usually generated with an (almost) constant magnitude but different vector orientations to cover all possible spherical angles.

This "thin-shell" calibration procedure employed with the SANSA Helmholtz coil system uses the spherical harmonic analysis method (SHM), and is described in detail by Risbo [2001, 2003]. The magnetometer is currently aligned with the coil system using a laser beam aligned to the magnetic axes of the coil system, reflecting off a mirror attached to magnetometer enclosure. The resulting "sphere" of magnetic field vectors are decomposed using SHM and least squares minimization. The result is a 3×3 matrix related to magnetometer body-frame containing the $\mathbf{A} = \mathbf{R}^{-1}\,\mathbf{P}^{-1}\,\mathbf{S}^{-1}$ matrix.

To obtain non-orthogonal angles from the **A** matrix, we used "QR" decomposition to obtain the orthogonal and upper triangular matrix [Anderson 1992]. To obtain the $\mathbf{P}^{-1}$ components, we also used the "scalar-calibration" procedure described in Olsen [2003] on the same thin-shell data (omitting the **R** matrix). In this method, the minimization criteria to find the $\mathbf{P}^{-1}\mathbf{S}^{-1}$ matrix (or its components) is the root-mean-square-error RMSE between the scalar magnitude of the applied vector in the coil system $\mathrm{b}_{sca}=\|\mathbf{b}_{coil}\|$ and the scalar magnitude of estimated vector $\|\mathbf{b}_{mag}\|$:

$$\mathrm{RMSE} = \sqrt{\frac{1}{N-1}\sum_i^N(\|\mathbf{b}_{mag}(\mathrm{i})\| - \mathrm{b}_{sca}(\mathrm{i}))^2} \quad (4)$$

We verified our results with a different calibration procedure, which is described in Brauer [1999], and Merayo [1999] and we did not find any significant difference in the results of these methods.

III. ANGULAR CALIBRATIONS

A. Calibration Results

The results were obtained on a single magnetometer type LEMI-011B [ISR Lviv 2019], serial numbers 319 and 379, respectively – see Table 1. The angles, obtained by the method of Olsen [2003], were compared to a direct measurement using an Askania circle with about ±1.5' = 2.5×10^{-2} degrees accuracy, and with a two-axis tilting jig with modified optical encoders (Heidenhain ERO-1324-3600, estimated total system accuracy about ±100" = 3×10^{-2} degrees) – see Fig. 4. The direct measurements were done by minimizing response at the respective axis when energizing the orthogonal coil (by rotation/tilting), and then doing the same for the second axis in pair.

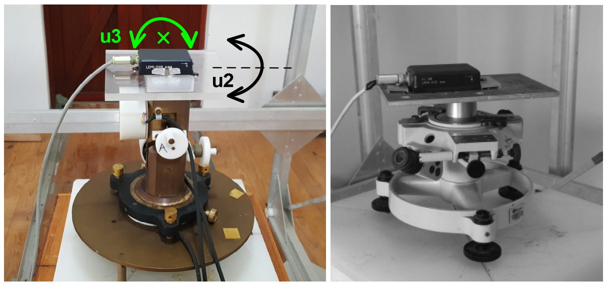

Fig. 4. The tilting jig with optical encoders for u_2 and u_3 measurements (left), Askania circle for horizontal u_1 angle estimation (right).

Table 1. Results of angular deviation measurements

	u_1 [°]	u_2 [°]	u_3 [°]	remark
LEMI-011B #319				
08/2013	-1.71	-0.51	4.94	5 years old
22/10/2018	-1.68	-0.47	4.83	
22/10/2018	-1.64	-0.53	4.75	direct meas.
24/10/2018	-1.68	-0.47	4.84	
LEMI-011B #379				
05/2017	1.39	-1.42	-0.84	1 year old
15/10/2018	1.38	-1.42	-0.85	
18/10/2018	1.39	-1.41	-0.87	
18/10/2018	1.33	-	-	direct
19/10/2018	*1.41*	*-1.36*	*-0.94*	*coils misaligned*
20/10/2018	*1.42*	*-1.37*	*-0.93*	
22/10/2018	*1.41*	*-1.37*	*-0.94*	
22/10/2018	*-*	*-1.32*	*-0.90*	*direct meas.*

We can see that the short-time spread of calculated angles of

This is the author's version of an article that has been published in this journal. Changes were made to this version by the publisher prior to publication.
The final version of record is available at http://dx.doi.org/10.1109/LMAG.2019.2944125

about ±0.01° (LEMI-011B #319) increases up to 0.1° for the 5-year period, which is more than anticipated. Also, the comparison to the direct measurement was within 0.1°, although the instruments are by far more accurate. In the next section, we will try to derive the sources of this uncertainty. It is evident that the coil calibration is an issue, which can be seen in the LEMI-011B #379 results - on 19/10/2018 the coils have been misaligned accidentally, which manifested itself in the angular calibration results.

We could verify the coil misalignment by doing a subsequent calibration of the coil system with an Overhauser magnetometer using a modified scalar-calibration procedure [Olsen 2003]. Further details are found in [Risbo 2003, p. 677]. The non-orthogonality of the coils was up to 6×10^{-2} degree and could be suppressed below 3×10^{-4} degree with the abovementioned recalibration - see Table 2.

Table 2. Result of coil system re-calibration

	u1 [°]	u2 [°]	u3 [°]
before cal. 10/2018	9.7×10^{-3}	6.4×10^{-2}	2.6×10^{-3}
after cal. 07/2019	2×10^{-4}	-3×10^{-4}	0

B. Estimating the Uncertainty

To establish the uncertainty of our calibration, we performed fifteen consecutive test runs and calculations on a single sensor - the space-qualified LEMI-011S (Fig. 1). The resulting histogram for the estimation of the three angles is shown in Fig. 5 - standard deviation was found below 6.6×10^{-4} degree. As the measurements were performed over a 12-hour span, these statistics also cover the effects of on-site noise and imperfections of the Earth's field cancellation in the coil system. We can consider the standard deviation as a type-A measurement uncertainty U_A [JGCM 2008].

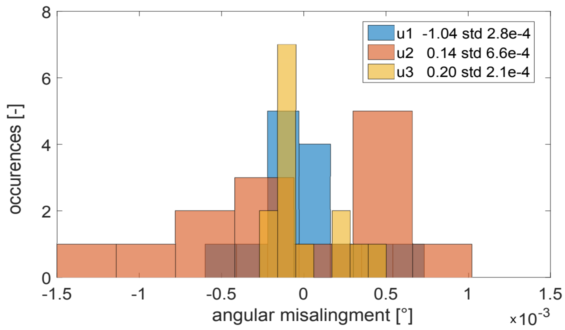

Fig. 5. Histogram with average values and the standard deviation for the calculated non-orthogonal angles (LEMI-011S, 15 runs).

As shown previously, we can experience coil non-orthogonality and its instability - see Table 2. This would be the source of type-B calibration uncertainty U_B for both the thin-shell method and direct measurement. The combined uncertainty U (k=2, 95% probability coverage) is then [JGCM 2008]:

$$U = 2\sqrt{{U_A}^2 + {U_{Bcoils}}^2 + {U_{Binst}}^2} \qquad (5)$$

where U_{Bcoils} is the type-B measurement uncertainty due to coils calibration, U_A is the standard deviation of the results calculated above and U_{Binst} is the uncertainty of the instrument used in the direct comparison if applicable (either Askania or tilting device).

For numeric calculations from the thin-shell run, we assume the worst-case observed standard deviation being U_B and coil misalignment with assumed triangular distribution being U_A:

$$U_{calc} = 2\sqrt{(6.6\times10^{-4})^2 + \left(\frac{0.064}{\sqrt{6}}\right)^2} = 5.2\times10^{-2} \qquad (6)$$

For the direct measurement, where we have the instrument uncertainty in addition (assuming a uniform distribution of scale error), thus we can write:

$$U_{meas} = 2\sqrt{(6.6\times10^{-4})^2 + \left(\frac{0.064}{\sqrt{6}}\right)^2 + \left(\frac{0.03}{\sqrt{3}}\right)^2} = 6.2\times10^{-2} \qquad (7)$$

In Fig. 6, the calculation and measurement results for u_2 on LEMI-011B #379 are plotted, together with uncertainties. The other angles are not displayed because of similarity of the results. We see that our measurements of u_2 fit well within the established uncertainty.

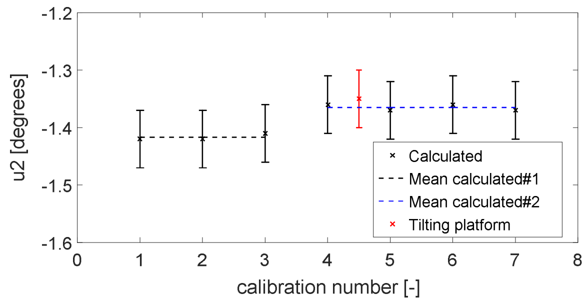

Fig. 6. Calculated u_2 angles (black) with their mean values, together with direct measurement on tilting platform (red). The 4 points on the right are after the coil calibration changed. LEMI-011B #379 used.

C. Statistics on a single magnetometer type

We demonstrate the necessity of angular calibrations on the example of a set of 57 magnetometers (LEMI-011B). From the results in Fig. 7 we see that the datasheet value [LEMI011B] of max. 2° non-orthogonality is met within one standard deviation. The maximum observed value was +4.5 °. This is due to the fact that the precise fluxgate magnetometer sensors are mostly hand-assembled.

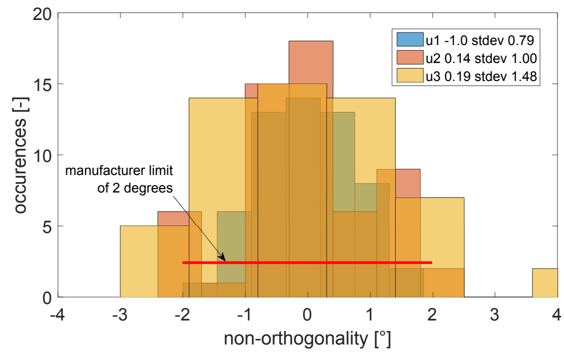

Fig. 7. Statistics on single magnetometer type (LEMI-011B); 57 pieces tested.

IV. BODY-FRAME RELATED CALIBRATIONS

A. Current method

The alignment of the DUT to the global (coil frame) is performed with a laser aligned to the magnetic axis of the horizontal coil and a precise mirror glued to the magnetometer body. This requires a skilled operator, thus we propose a novel method for body-frame calibration.

B. Proposed procedure

The procedure relies on magnetometer calibration in 4 (or even just 3) particular attitudes. The first sensor attitude can be arbitrarily chosen. The three remaining are attitudes with the sensor rotated along its body axis X, Y, Z respectively - see Fig. 8. In each step, a thin-shell calibration is performed and a rotation matrix $\mathbf{R}$ is obtained from the calibration matrix result (by QR decomposition).

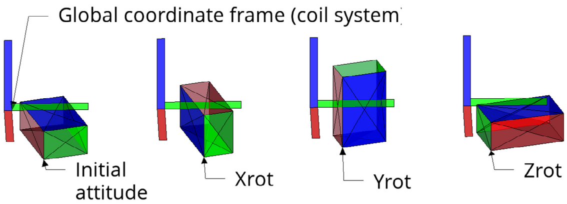

Fig. 8. 4-step rotation to obtain body-frame-referenced calibration.

The rotation matrix from the initial (aligned) position to the first arbitrary position can be written as $\mathbf{R}_0 = \mathbf{R}_{BG}\mathbf{I}\mathbf{R}_{SB}$, where $\mathbf{R}_{SB}$ represents the sensor to body frame rotation, $\mathbf{R}_{BG}$ is the body frame to global frame (=coil frame) rotation and $\mathbf{I}$ is unit matrix. The next rotation matrix to a different attitude after rotation in body frame is $\mathbf{R}_g = \mathbf{R}_{BG}\mathbf{R}_i\mathbf{R}_{SB}$. We can then obtain the relative rotation $\mathbf{Q}$ between the two attitudes $\mathbf{R}_0$ and $\mathbf{R}_g$ as follows:

$$\mathbf{Q}_i = \mathbf{R}_0^T\mathbf{R}_i = \mathbf{R}_{SB}^T\mathbf{R}_i^T\mathbf{R}_{SB} \quad (8)$$

The eigenvector $\mathbf{v}_x$ of relative rotation describes the axis of rotation in reference to a sensor frame:

$$\mathbf{v}_x = \mathrm{eigvec}(\mathbf{Q}_x) = \mathbf{R}_{SB}^T\mathrm{eigvec}(\mathbf{R}_x^T) \quad (9)$$

Then the rows of rotation matrix $\mathbf{R}_{SB}$ rows are the eigenvectors of relative rotations:

$$\mathbf{v}_x = \mathbf{R}_{SB}^T[1\ 0\ 0]^T$$
$$\mathbf{R}_{SB}^T = [\mathbf{v}_x\ \mathbf{v}_y\ \mathbf{v}_z]^T$$

The angles of rotations do not have to be precise as long as the rotation axes are perpendicular. Due to arithmetic imprecision and mostly due to imperfections of rotations axis attitudes it is better to create $\mathbf{R}_{SB}$ from each pair of eigenvectors and to calculate the third vector to form a normal basis each time. The spread of rotation angles between each calculated matrix can then be used to evaluate the results. A similar approach to the extraction body frame related calibration is described by Primdahl [2002].

The main advantage of using the reference plane and block to perform the rotation is that once the 4-step method is executed for one magnetometer, the reference plane/block (in arbitrary attitude) is also calibrated at the same time. After that, only 1-step calibration in the initial position can be used to calibrate other magnetometers, which saves time and reduces possibilities of human error.

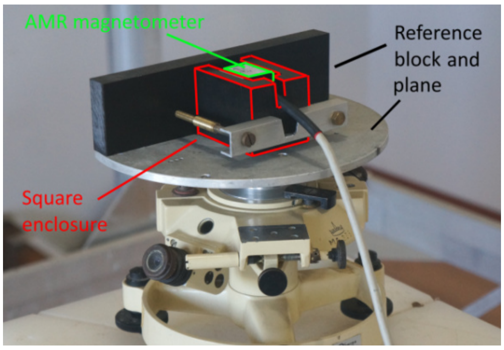

Fig. 9. The magnetometer (triaxial AMR) is fitted in a square enclosure mounted to the reference block and plane.

C. Procedure verification

We verified the procedure using a triaxial AMR magnetometer [Novotny 2018] mounted with respect to the reference block and plane - see Fig. 9. The magnetometer in its square enclosure was then rotated according to Fig. 8, the $\mathbf{R}_{SB}$ matrices were calculated and the Euler angles for the sensor-frame-to-body-frame rotation (SF2BF) and global-frame-to-body-frame (GF2BF) were established.

In Table 3, results for three different initial attitudes (rotation in azimuth about 0, 20 and 60°) are shown. Ideally, the results would be the same. Z, Y' and X" are the Euler angles in this order.

Table 3. Results of the proposed procedure

SF2BF	**Z [°]**	**Y‘ [°]**	**X‘‘ [°]**
initial 0°	-0.90 ±0.01	-0.52 ±0.03	-0.34 ±0.03
initial 20°	-0.94 ±0.04	-0.55 ±0.01	-0.22 ±0.09
initial 60°	-0.96 ±0.04	-0.55 ±0.01	-0.23 ±0.10
mean value	-0.93 ±0.04	-0.54 ±0.02	-0.27 ±0.09
GF2BF diff.	-0.01 ±0.04	0.08 ±0.03	0.01 ±0.11

The last row are the differences between alignment to the coil axes as obtained by the current method (leveling and laser alignment) and the new method. We see that both methods agree within 0.1°.

V. CONCLUSION

We show that our one-year expanded (k=2) uncertainty of angular deviation calibrations is about 6×10^{-2} degrees of arc which we found as the coil-system non-orthogonality, which can improve down to 3×10^{-4} degrees with a numerical coil re-calibration. The numerical results were comparable with direct measurements within this uncertainty. We also see that with hand-assembled fluxgate magnetometers, it is crucial to calibrate the orthogonal angles.

The proposed method to obtain body-frame related magnetometer calibration was verified. Its advantage is not only time-saving, but avoiding of tilting and leveling of the device under test, to align it with the coil system, which brings further uncertainties. Even with a non-ideal reference block and magnetometer enclosure, the body-frame referenced calibration resulted in a spread of ± 0.1°. Also, the agreement to the current procedure with leveling and laser alignment is within 0.1°, which also corresponds to inclinometer resolution. In order to improve the results, a more precisely machined reference block and reference enclosure is required – with 10 µm manufacturing precision, 6×10^{-3} degrees would be possible.

ACKNOWLEDGMENT

This work was supported in part by the Czech Technical University through the Ministry of Education mobility grant "International Mobility of Researchers in CTU", No CZ.02.2.69/0.0/0.0/16_027/0008465.

REFERENCES

Anderson E, Bai Z, Dongarra J (1992), "Generalized QR factorization and its applications", *Linear Algebra and its Applications*, vol. 162, pp. 243-271, doi: 10.1016/0024-3795(92)90379-O

Bonnet S, Bassonpierre C, Godin C, Lesecq S, Barraud A (2009), "Calibration methods for inertial and magnetic sensors", *Sensors and Actuators A: Physical*, vol. 156(2), pp. 302–311, doi:10.1016/j.sna.2009.10.008

Brauer P, Merayo J M G, Risbo T, Primdahl F (2001), "Magnetic calibration of vector magnetometers: linearity, thermal effects and stability", *ESA Conference proceedings SP-490*, Ground and In-Flight Space Magnetometer Calibration Techniques.

Dietrich M R, Bailey K G, O'Connor T P (2017), "Alignment of a vector magnetometer to an optical prism", *Review of Scientific Instruments*, vol. 88(5), id. 055105, doi:10.1063/1.4983146

Figaro D, Bryant T, Boeen A (2011), "Spherical calibration and reference alignment algorithms", Patent No: 7930148, http://www.freepatentsonline.com/7930148.html

ISR Lviv (2019), "Super-low-power three-componenhts flux-gate magnetometer LEMI-011", National Space Agency of Ukraine and National Academy of Sciencese of Ukraine, accessed: 20.8.2019, https://www.isr.lviv.ua/lemi011.htm

JGCM Joint Committee for Guides in Metrology (2008) "Evaluation of measurement data—Guide to the expression of uncertainty in measurement," Geneva: International Organization for Standardization, ISBN 926710188-9, https://www.bipm.org/utils/common/documents/jcgm/JCGM_100_2008_E.pdf

Merayo J M G, Brauer P, Primdahl F, Petersen J R (1999), "Absolute magnetic calibration and alignment of vector magnetometers in the Earth's magnetic field", *ESA Conference proceedings SP-490*, Ground and In-Flight Space Magnetometer Calibration Techniques.

Novotný D, Petrucha V, Janošek M (2018), "A Digitally Compensated AMR Magnetometer," *IEEE Transactions on Magnetics*, vol. 55, issue 1, id. 4000805, doi:10.1109/TMAG.2018.2873235.

Olsen N, Tøffner-Clausen L, Sabaka T J, Brauer P, Merayo J M G, Jørgensen J L, Léger J –M, Nielsen O V, Primdahl F, Risbo T (2003), "Calibration of the Ørsted vector magnetometer," *Earth, planets and space*, vol. 55, pp. 11-18, doi: 10.1186/BF03352458

Pajunpää K, Klimovich E Y, Korepanov V, Posio P, Nevalinna H, Schmidt W, Genzer M, Harri A –M, Lourenço A M F (2007), "Accredited Vector Magnetometer Calibration Facility", *Geophysica*, vol. 43(1–2), pp. 59–76.

Primdahl F, Brauer P, Merayo J M G, Petersen J R, Risbo T (2002), "Determining the direction of a geometrical/optical reference axis in the coordinate system of a triaxial magnetometer sensor", *Measurement Science and Technology*, vol. 13(12), pp. 2094–2098, doi:10.1088/0957-0233/13/12/339

Risbo T, Brauer P, Merayo J M G, Nielsen O, Petersen J R, Primdahl F, Olsen N (2002), "Ørsted calibration mission: The thin shell method and the spherical harmonic analysis", *ESA Conference proceedings SP-490*, Ground and In-Flight Space Magnetometer Calibration Techniques.

Risbo T, Brauer P, Merayo J M G, Nielsen O V, Petersen J R, Primdahl F, Richter I (2003), "Ørsted pre-flight magnetometer calibration mission," *Meas. Sci. Technol.*, vol. 14(5), pp. 674, doi: 10.1088/0957-0233/14/5/319

Vcelak J (2009), *Application of magnetic sensors for navigation systems*, Aachen: Shaker Verlag, ISBN 3832277382, pp. 77-98.